Electronic States of Cyclobutadiene Heteroanalogues. Critical Biradicaloids

Vlasta Bonačić-Koutecký,*[1a] Klaus Schöffel,[1a] and Josef Michl[1b]

Contribution from the Institut für Physikalische und Theoretische Chemie, Freie Universität Berlin, Takustrasse 3, 1000 Berlin 33, West Germany, and Center of Structure and Reactivity, Department of Chemistry, The University of Texas at Austin, Austin, Texas 78712-1167.
Received November 22, 1988

Abstract: The S_0–S_1 and S_0–T_1 energy gaps obtained from large-scale CI calculations for SCF- or CASSCF-optimized geometries of donor–acceptor push–pull substituted cyclobutadienes behave as predicted from the simple two-electron two-orbital model. For a particular electronegativity difference between atoms in the two pairs of diagonally opposed positions, the S_0–S_1 energy gap almost vanishes. This occurs in the case of "critical biradicaloids". An example is protonated azacyclobutadiene at nonequilibrium geometries accessible on the lowest potential energy surface at energies comparable to activation energies of fast thermal reactions. In strongly heterosymmetric biradicaloids such as 1,3,2,4-diazadiboretidine, the S_0–S_1 gap is larger, S_1 and T_1 states are of charge-transfer nature, and the S_1–T_1 energy gap is negative. The observed absorption band of tri-*tert*-butylazacyclobutadiene has been assigned to an $n\pi^*$ transition. The application of the concept of critical biradicaloids to photochemical 2s + 2s cycloaddition has been discussed.

The formal relation of the extremely reactive cyclobutadiene[2] (*1*) to its stable "push–pull" stabilized derivatives[3] and related heterocycles[4] containing donors in one set of diagonally opposed positions and acceptors in the other was anticipated theoretically[5] and has been discussed in some detail.[6,7] On the basis of a consideration of a simple model and results of preliminary calculations, we have suggested more recently[8] that the electronic states of more moderately push–pull perturbed cyclobutadiene should possess very interesting properties ("critical biradicaloids"). Presently, we report the full results of calculations of 1–6 (Chart I) performed for optimized molecular geometries, using large CI expansions.

Computational Procedures

The calculations were performed with the 4-31G basis set. Geometry optimization was done at the SCF level for **1–6** and at the CASSCF (complete active space self-consistent field) level for **1** using the analytic gradient method.[9] At the optimized geometry, two separate multireference direct CI calculations with singly and doubly excited configurations[10] (MR-SD-CI) were performed for the singlet states and one for the triplet state ($0.5–5 \times 10^5$ configurations each). The criterion for inclusion of a reference configuration was a squared coefficient equal to at least 0.0025 in a single-reference SD–CI calculation. One of the singlet CI calculations started with the closed shell (CS) and the other with open-shell (OS) RHF orbitals. For symmetries higher than C_s, the two CI calculations produce states of different symmetries. At C_s geometries, the direct CI was well-behaved for the lowest singlet state but not for the next higher singlet, which is of the same symmetry. Its energy was therefore obtained with the MRD–CI procedure[11] using iterative natural orbitals. For the lowest singlet, the direct CI and the MRD–CI procedures yielded almost identical results. In cases of particular interest (small S_0–S_1 gap), the calculations were repeated at the above geometries

Chart I

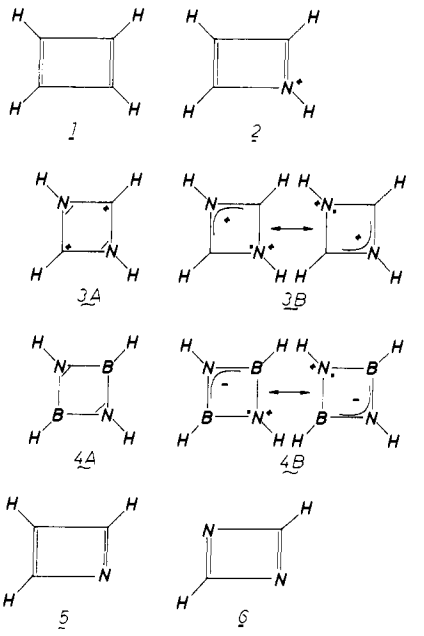

Table I. Singlet and Triplet States of Cyclobutadiene

sym constraints	state sym	E(SCF)[a]	E(CI)[a]	WF[b]	ΔE[c]
D_{2h}[d]	^1A_g	−0.484 57[e]	−0.771 02[f]	$^1\|b^2\rangle$	
	2^1A_g		−0.629 06[f]	$^1\|a^2\rangle$	89.1
	$^3B_{1g}$	−0.383 55	−0.729 83[f]	$^3\|ab\rangle$	25.85

[a] The reference energy is −153 au. [b] Leading configuration in the CI wave function. Lower case letters label delocalized MO's. [c] The CI energy difference with respect to the lowest ground-state energy in kilocal per mole. [d] The geometry to which the positions of nuclei have been constrained in CASSCF geometry optimization. [e] CASSCF energy. [f] MRD–CI calculations (6 references/2 roots).

(1) (a) Freie Universität Berlin. (b) The University of Texas at Austin.
(2) Maier, G. *Angew. Chem., Int. Ed. Engl.* **1988**, *27*, 309. Bally, T., Masamune, S. *Tetrahedron* **1980**, *36*, 343. Arnold, B.; Michl, J. In *Kinetics and Spectroscopy of Carbenes and Biradicals*; Platz, M., Ed.; Plenum: New York, in press.
(3) Gompper, R.; Seybold, G. In *Topics in Non-benzenoid Aromatic Chemistry*; Nozoe, T., Breslow, R., Hafner, K., Ito, S., Murata, I., Eds.; Hirokawa, Tokyo, 1977; Vol. II. Gompper, R.; Kroner, J.; Seybold, G.; Wagner, H. U. *Tetrahedron* **1976**, *32*, 629.
(4) Paetzold, P.; Schröder, E.; Schmid, G.; Boese, R. *Chem. Ber.* **1985**, *118*, 3205.
(5) Hoffmann, R. *Chem. Commun.* **1969**, 240.
(6) Baird, N. C. *Inorg. Chem.* **1973**, *12*, 473.
(7) Borden, W. T., Ed. *Diradicals*; Wiley: New York, 1982; p 60.
(8) Bonačić-Koutecký, V.; Koutecký, J.; Michl, J. *Angew. Chem. Int. Ed. Engl.* **1987**, *26*, 170. Michl, J.; Bonačić-Koutecký, V. *Tetrahedron* **1988**, *44*, 7559.
(9) Guest, M. F., Wilson, S. Presented at the 180th National Metting of the American Chemical Society Las Vegas, NV, August 1980.
(10) Saunders, V. R.; Guest, M. F. *Comput. Phys. Commun.* **1982**, *26*, 389. Guest, M. F. Supercomputer Simulations in Chemistry, Montreal, 1985. Saunders, V. R.; van Lenthe, J. H. *Mol. Phys.* **1983**, *48*, 923.
(11) Buenker, R. J.; Peyerimhoff, S. D. *Theor. Chim. Acta* **1974**, *35*, 33. Buenker, R. J.; Peyerimhoff, S. D.; Butscher, W. *Mol. Phys.* **1978**, *35*, 771. Buenker, R. J. In *Studies in Physical and Theoretical Chemistry: Current Aspects of Quantum Chemistry*; Carbo, R. T., Ed.; Elsevier: Amsterdam, The Netherlands, 1982; Vol. 21, p 17.

0002-7863/89/1511-6140$01.50/0

Table II. Singlet and Triplet States of Protonated Azacyclobutadiene **2**

sym constraints	SCF opt geom S(CS) state sym	E(SCF)[a]	E(Cl)[a]	WF[b]	ΔE[c]	S(OS) state sym	E(SCF)[a]	E(Cl)[a]	WF[b]	ΔE[c]	T(OS) state sym	E(SCF)[a]	E(Cl)[a]	WF[b]	ΔE[c]
C_s[d]	^{1}A′	−0.745 00	−1.100 54 (−1.103 41[e])	$^1\|b^2\rangle$		^{1}A′		(−1.099 37[e])	$^1\|b^2\rangle$	0.74	≡C_{2v}				
	2^1A′		(−0.976 96[e])	$^1\|ab\rangle$	77.55	2^1A′		(−1.028 33[e])	$^1\|ab\rangle$	47.10					
	^{3}A′	−0.668 69	−1.008 25	$^3\|ab\rangle$	57.91										
C_{2v}[d]	^{1}A$_1$	−0.731 10	−1.073 45	$^1\|B^2\rangle$	17.00	^{1}A$_1$	−0.711 11	−1.055 20	$^1\|B^2\rangle$	28.45					
	^{1}B$_1$	−0.705 18	−1.079 21	$^1\|AB\rangle$	13.38	^{1}B$_1$	−0.715 65	−1.086 21	$^1\|AB\rangle$	8.99					
						^{3}B$_1$	−0.740 04	−1.081 71	$^3\|AB\rangle$	11.82	^{3}B$_1$	−0.741 45	−1.083 60	$^3\|AB\rangle$	10.63
"D_{4h}"[d]	^{1}A$_1$	−0.725 65	−1.067 69	$^1\|B^2\rangle$	20.61	^{1}B$_1$	−0.707 56	−1.083 76	$^1\|AB\rangle$	12.31	^{3}B$_1$	−0.736 5	−1.080 06	$^3\|AB\rangle$	12.85

[a] The reference energy is −169 au. [b] Leading configuration in the CI wave function. Lower and upper case letters label delocalized and localized MO's, respectively. [c] The CI energy difference in kilocalories per mole with respect to the lowest ground-state energy. [d] The geometry to which the positions of nuclei have been constrained. [e] MRD-CI calculations with natural orbitals as one-electron functions for each root and several iterations.

Table III. Singlet and Triplet States of Protonated 1,3-Diazacyclobutadiene **3**

sym constraints	S(CS) state sym	E(SCF)[a]	E(Cl)[a]	WF[b]	ΔE[c]	S(OS) state sym	E(SCF)[a]	E(Cl)[a]	WF[b]	ΔE[c]	T(OS) state sym	E(SCF)[a]	E(Cl)[a]	WF[b]	ΔE[c]
	^{1}A$_{1g}$	−0.814 70	−1.162 21	$^1\|B^2\rangle$		^{1}B$_{1g}$	−0.735 9	−1.137 88	$^1\|AB\rangle$	15.27					
"D_{4h}"	^{3}B$_{1g}$	−0.740 87	−1.114 20	$^3\|AB\rangle$	30.13						^{3}B$_{1g}$	−0.741 60	−1.118 77		27.26
D_{2h}[d]		≡"D_{4h}"				^{1}A$_g$	−0.809 71	−1.157 90	$^1\|B^2\rangle$	2.74					
						^{1}B$_{1g}$	−0.737 84	−1.138 76	$^1\|AB\rangle$	14.72	^{3}B$_{1g}$	−0.743 89	−1.120 93		25.90
C_{2v}[d]		≡"D_{4h}"				^{1}B$_1$	−0.745 80	−1.133 97	$^1\|AB\rangle$	17.72	^{3}B$_1$	−0.750 73	−1.117 95		27.77

[a] Reference energy is −185 au. [b-f] Compare Table II.

Table IV. Singlet and Triplet States of 1,3,2,3-Diazadiboretidine

sym constraints	S(CS) state sym	E(SCF)[a]	E(Cl)[a]	WF[b]	ΔE[c]	S(OS) state sym	E(SCF)[a]	E(Cl)[a]	WF[b]	ΔE[c]	T(OS) state sym	E(SCF)[a]	E(Cl)[a]	WF[b]	ΔE[c]
D_{2h}[d]	^{1}A$_g$	−0.457 54	−0.762 35	$^1\|B^2\rangle$		^{1}A$_g$	−0.446 39	−0.753 42	$^1\|B^2\rangle$	5.60					
	^{1}B$_{1g}$	−0.268 34	−0.617 27	$^1\|AB\rangle$	91.04	^{1}B$_{1g}$	−0.279 11	−0.630 78	$^1\|AB\rangle$	82.56					
	^{3}B$_{1g}$	−0.275 14	−0.604 84	$^3\|AB\rangle$	98.84	^{3}B$_{1g}$	−0.285 54	−0.618 18	$^3\|AB\rangle$	90.47	^{3}B$_{1g}$	−0.285 56	−0.618 97	$^3\|AB\rangle$	89.97
C_{2v}[d]		≡D_{2h}				^{1}B$_1$	−0.291 28	−0.623 91	$^1\|AB\rangle$	86.87	^{3}B$_1$	−0.297 30	−0.615 18	$^3\|AB\rangle$	92.35
"D_{4h}"[e]	^{1}A$_g$	−0.454 65	−0.759 55	$^1\|B^2\rangle$	1.78	^{1}B$_{1g}$	−0.280 70	−0.627 34	$^1\|AB\rangle$	84.72	^{3}B$_{1g}$	−0.280 80	−0.614 52	$^3\|AB\rangle$	92.76

[a] Reference energy is −160 au. [b-f] Compare Table II.

Table V. Singlet and Triplet States of Azacyclobutadiene **5**

SCF constraints	S(CS) state sym	E(SCF)[a]	E(Cl)[a]	WF[b]	ΔE[c]	S(OS) state sym	E(SCF)[a]	E(Cl)[a]	WF[b]	ΔE[c]	T(OS) state sym	E(SCF)[a]	E(Cl)[a]	WF[b]	ΔE[c]
C_s[d]	^{1}A′	−0.366 86	−0.745 09 (−0.743 03[f])	$^1\|b^2\rangle$		^{1}A′	−0.362 04	(−0.720 89[f])	$^1\|ab\rangle$	15.19					
	^{1}A″	−0.253 57	−0.599 20	$^1n\pi^*$	91.50										
	2^1A′		(−0.566 29[f])	$^1\|ab\rangle$	112.20	2^1A′		(−0.650 5[f])	$^1\|b^2\rangle$	59.36					
	^{3}A′	−0.307 27	−0.662 88	$^3\|ab\rangle$	51.64						^{3}A′	−0.362 24	−0.715 59	$^3\|ab\rangle$	18.5
C_{2v}[d]	^{1}A$_1$	−0.325 11	−0.675 96	$^1\|B^2\rangle$	43.38	^{1}A$_1$	−0.315 72	−0.660 70	$^1\|B^2\rangle$	52.96					
	^{1}B$_1$	−0.352 57	−0.729 32	$^1\|AB\rangle$	9.90	^{1}B$_1$	−0.361 76	−0.732 73	$^1\|AB\rangle$	7.36					
						^{3}B$_1$	−0.368 10	−0.716 34	$^3\|AB\rangle$	18.04	^{3}B$_1$	−0.368 18	−0.719 12	$^3\|AB\rangle$	16.3
"D_{4h}"[e]	^{1}A$_1$	−0.305 82	−0.654 09	$^1\|B^2\rangle$	57.10	^{1}B$_1$	−0.355 33	−0.730 38	$^1\|AB\rangle$	9.23	^{3}B$_1$	−0.362 71	−0.713 25	$^1\|AB\rangle$	19.98

[a] Reference energy is −169 au. [b-f] Compare Table II.

Table VI. Singlet and Triplet States of 1,3-Diazacyclobutadiene **6**

sym constraints	S(CS) state sym	E(SCF)[a]	E(Cl)[a]	WF[b]	ΔE[c]	S(OS) state sym	E(SCF)[a]	E(Cl)[a]	WF[b]	ΔE[c]	T(OS) state sym	E(SCF)[a]	E(Cl)[a]	WF[b]	ΔE[c]
C_s[d]	^{1}A′	−0.324 70	−0.715 46 (−0.714 56)[f]	$^1\|b^2\rangle$		^{1}A′	−0.309 22	(−0.681 20[f])	$^1\|b^2\rangle$	21.50					
	^{1}A″	−0.220 02	−0.608 73	$^1n\pi^*$	66.98										
	2^1A′		(−0.535 38)[f]	$^1\|ab\rangle$	112.74	2^1A′		−0.632 90	$^1\|ab\rangle$	51.81					
	^{3}A′	−0.230 22	−0.612 84		64.40						^{3}A′	−0.314 35	−0.674 82	$^3\|ab\rangle$	23.24
C_{2v}[d]			≡D_{2h}			^{1}B$_1$	−0.308 44	−0.694 55	$^1\|AB\rangle$	13.12					
D_{2h}[d]	^{1}A$_g$	−0.294 99	−0.668 11	$^1\|B^2\rangle$	29.71	^{1}A$_g$	−0.286 62	−0.652 96	$^1\|B^2\rangle$	39.2					
	^{1}B$_{1g}$	−0.296 33	−0.692 35	$^1\|AB\rangle$	14.50	^{1}B$_{1g}$	−0.304 06	−0.697 67	$^1\|AB\rangle$	10.60					
						^{3}B$_{1g}$	−0.310 38	−0.679 38	$^3\|AB\rangle$	22.60	^{3}B$_{1g}$	−0.310 40	−0.680 62	$^3\|AB\rangle$	21.86
"D_{4h}"[e]	^{1}A$_g$	−0.260 48	−0.625 71	$^1\|B^2\rangle$	55.75	^{1}B$_{1g}$	−0.294 81	−0.687 27	$^1\|AB\rangle$	17.90	^{3}B$_{1g}$	−0.301 15	−0.670 18	$^3\|AB\rangle$	28.41

[a] Reference energy is −185 au. [b-f] Compare Table II.

using a 6-31**G basis set, but no significant changes resulted.

The results of the calculations are collected in Tables I–VI and Figures 1–7. For each compound, the geometry optimization was performed under each of the following four symmetry constraints: "D_{4h}" (C_{2v} square), D_{2h} (diamond or rectangle), C_{2v} (kite or trapezoid), and C_s (planar). For our purpose out-of-plane distortions were not interesting and were not examined. In each case, the optimization was done once for an open-shell T(OS) triplet wave function $^3|ab\rangle$, once for an S(OS) singlet wave function $^1|ab\rangle$ and once for a closed-shell S(CS) singlet wave function $^1|b^2\rangle$, using the restricted Hartree–Fock method. The resulting SCF approximations to the T_1, S_0, and S_1 states represented the leading term in the large CI expansion that was performed next. As expected from orbital degeneracy, more than one leading term in the calculation of singlet states appears only in the case of **1** at D_{4h} geometry. Therefore, the CASSCF method has been used in geometry optimization of **1**. Under constraints imposed by C_s symmetry the molecules **1**, **2**, **5**, and **6** adopted a rectangular or nearly rectangular shape with strongly alternating bond lengths in the ground state, whereas **3** and **4** adopted a square and rhombic shape, respectively (Chart I).

There is now good theoretical[12-15] and experimental[12,16] evidence in

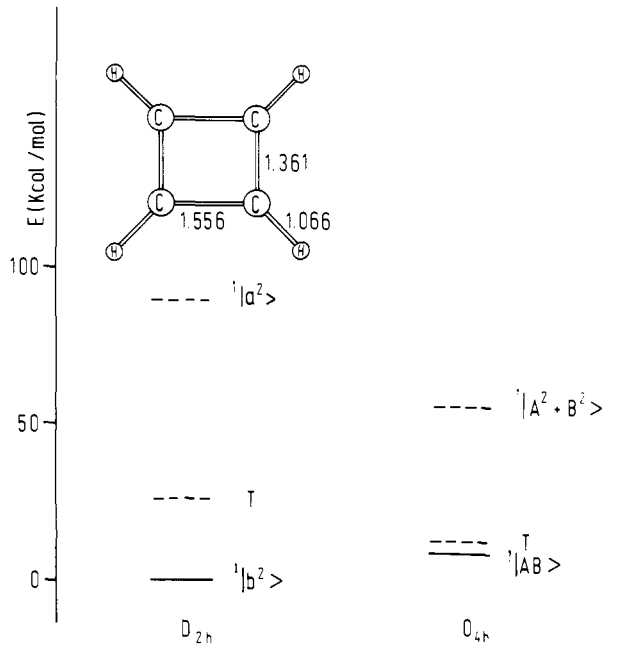

Figure 1. CASSCF geometry of **1** (optimized under D_{2h} symmetry constraints) and CI energies for S_0, S_1, and T states at CASSCF-optimized D_{2h} and D_{4h} geometries (the CASSCF-optimized D_{4h} C–C bond length is 1.456 Å). See Table I.

favor of fairly rapid tunneling between the two rectangular structures in the parent **1**. However, it is slow on the IR time scale in **1**, and we assume that it will be slow on the even shorter time scale of electronic spectroscopy in **2–6**, so that we can ignore it in the following.

Results

In the following, we start by considering molecules **1–4** whose low-lying excited states are of the $\pi-\pi^*$ type. The simpler case of symmetrical geometries is taken up first; the results for C_s geometries are described next. Subsequently, we analyze the results for **5** and **6**, complicated by the presence of low-energy $n\pi^*$ states.

Cyclobutadiene (1) and Its Protonated Heteroanalogues. Symmetrical Geometries. At square-, kite-, and diamond-shaped geometries, the two nonbonding MO's have the localized form $|A\rangle$, $|B\rangle$, shown in Figure 8. One is situated along one diagonal, the other, along the other diagonal, and their relative energies are dictated by the relative electronegativities of the atoms located on the two diagonals. The more stable of the two orbitals is labeled $|B\rangle$. The wave functions $^1|A^2\rangle$ and $^1|B^2\rangle$ will be referred to as "hole-pair" configurations and $^1|AB\rangle$ and $^3|AB\rangle$ as "dot-dot" configurations. When A and B are each localized on a single center, these wave functions correspond very closely to valence-bond (VB) structures, but since in our case the A and B are delocalized over several centers we use the term "configurations".[8] The dot-dot configuration $^1|AB\rangle$ is antisymmetric (^{1}B), and the hole-pair configurations $^1|A^2\rangle$ and $^1|B^2\rangle$ are symmetric (^{1}A). Therefore, the former does not mix with the latter two.

In the large-scale CI wave function, the S_0 of **1** is dominated by the configuration $^1|AB\rangle$, the slightly less stable T_1 by $^3|AB\rangle$, the much higher S_1 state by the in-phase mixture of the hole-pair configurations, $^1|B^2\rangle + {}^1|A^2\rangle$, and the somewhat higher S_2 state by their out-of-phase mixture. In square **1**, the mixing of $^1|A^2\rangle$ and $^1|B^2\rangle$ is perfectly balanced (cf. Table I and Figure 1). The reasons for the S_0–T_1 state order and for the stabilization of the in-phase combination of $^1|B^2\rangle$ and $^1|A^2\rangle$ relative to the out-of-phase combination are now well understood.[17-20] The results agree qualitatively with other recent ab initio calculations on the excited states of cyclobutadiene.[21]

As one proceeds along the series **1–4** (Chart I, Tables I–4, and Figures 1–4), the introduction of electronegative heteroatoms causes orbital $|B\rangle$ and the configuration $^1|B^2\rangle$ to decrease in energy and the mixing of $^1|A^2\rangle$ and $^1|B^2\rangle$ is then no longer balanced. In **3** and **4** the large-scale CI wave functions for the S_0 state are totally dominated by the configuration $^1|B^2\rangle$. In **4**, this can be most simply represented by a structure with a lone pair on each nitrogen atom (**4A**), in complete agreement with the experimental stability of the tetra-*tert*-butyl derivative of **4**,[4] which contrasts with the high reactivity of **1**. This was anticipated a long time ago.[5]

The S_1 wave functions of **3** and **4** are dominated by $^1|AB\rangle$; that of **4** is quite high in energy (Figures 3 and 4). The charge distribution differs vastly from that of the S_0 state, since A and B are located in quite different regions of space. As a result, S_1 of **3** can be referred to as a "charge-translocation" excited state and that of **4** as a charge-transfer excited state ("charge-transfer biradicaloid"). The situation is symbolized in the valence-bond structures **3A** and **4A** for the S_0 states, while **3B** and **4B** are representative of the structures describing the S_1 states (Chart I).

Remarkably, the T_1 state of **3** and **4**, which is dominated by the $^3|AB\rangle$ configurations and is also of charge-translocation nature in **3** and charge-transfer nature in **4**, remains above the singlet dominated by the $^1|AB\rangle$ configurations, so that the state ordering now is the highly unusual S_0, S_1, and T_1 in the order of increasing energy ("negative" singlet–triplet splitting for the excited states). This type of behavior has also been computed for another strongly heterosymmetric biradicaloid, twisted aminoborane;[8,22] we are only aware of one case in which experimental evidence suggested that such an ordering might be present ([3.3.3]cyclazine[23]). However, it should be common in strongly twisted internal charge-transfer (TICT) species,[24] for which twisted aminoborane can be considered a prototype.

Since the states dominated by the $^1|B^2\rangle$ and $^1|AB\rangle$ configurations differ in symmetry and change their energetic order upon going from **1** to **4** they would clearly cross somewhere along the way if the electronegativity of the atoms along one of the diagonals in **2** could be changed continuously. At the crossing point, the biradicaloid would be "critically heterosymmetric".[8] The two components of its degenerate lowest singlet state S_0 and S_1 would still differ vastly in charge distribution, and T_1 might be expected to lie above both. Our effort to find such a critically symmetrical biradicaloid whose structure is intermediate between **1** and **4** has revealed that the protonated azacyclobutadiene **2** corresponds very closely to the crossing point. At the optimal square geometry for the lowest singlet state the S_0 wave function is dominated by the $^1|AB\rangle$ configuration and S_0 lies 10 kcal/mol below S_1, which is dominated by the $^1|B^2\rangle$ configuration. At the optimal kite geometry, S_0 is again dominated by $^1|B^2\rangle$ and now lies 19 kcal/mol below S_1, dominated by $^1|B^2\rangle$ (Figure 3). In both cases, T_1 lies a little above S_1 (Figure 2). At a kite geometry optimized for the S_1 state, the S_0–S_1 gap is only 3.5 kcal/mol. Clearly, within the accuracy of the present calculations, S_0 and S_1 of **2** are virtually degenerate at optimized symmetrical geometries.

Comparison with the 3 × 3 CI Model. The results obtained from the ab initio large-scale CI results are qualitatively just those

(12) Whitman, D. W.; Carpenter, B. K. *J. Am. Chem. Soc.* **1982**, *104*, 6473. Carpenter, B. K. *J. Am. Chem. Soc.* **1983**, *105*, 1700.
(13) Huang, M.-J.; Wolfsberg, M. *J. Am. Chem. Soc.* **1984**, *106*, 4039.
(14) Dewar, M. J. S.; Merz, K. M.; Jr.; Stewart, J. J. P. *J. Am. Chem. Soc.* **1984**, *106*, 4040.
(15) Carsky, P.; Bartlett, R. J.; Fitzgerald, G.; Noga, J.; Spirko, V. *J. Chem. Phys.* **1988**, *89*, 3008.
(16) Ordent, A. M.; Arnold, B. R.; Radziszewski, J. G.; Facelli, J. C.; Malsch, K. D.; Strub, H.; Grant, D. M.; Michl, J. *J. Am. Chem. Soc.* **1988**, *110*, 2648.
(17) Borden, W. T., Ed. *Diradicals*; Wiley: New York, 1982; p 41.
(18) Kollmar, H.; Staemmler, V. *J. Am. Chem. Soc.* **1977**, *99*, 3583.
(19) Gerhartz, W.; Poshusta, R. D.; Michl, J. *J. Am. Chem. Soc.* **1976**, *98*, 6427.
(20) Voter, A. F.; Goddard, W. A., III *J. Am. Chem. Soc.* **1986**, *108*, 2930.
(21) Ågren, H.; Correia, N.; Flores-Riveros, A.; Jensen, H. J. AA. *Int. J. Quantum Chem., Quantum Chem. Symp.* **1986**, *19*, 237.
(22) Bonačič-Koutecký, V.; Michl, J. *J. Am. Chem. Soc.* **1985**, *107*, 1765.
(23) Leupin, W.; Wirtz, J. *J. Am. Chem. Soc.* **1980**, *102*, 6068.
(24) Lippert, E.; Rettig, W.; Bonačič-Koutecký, V.; Heisel, F.; Miehé, A. *Adv. Chem. Phys.* **1987**, *68*, 173.

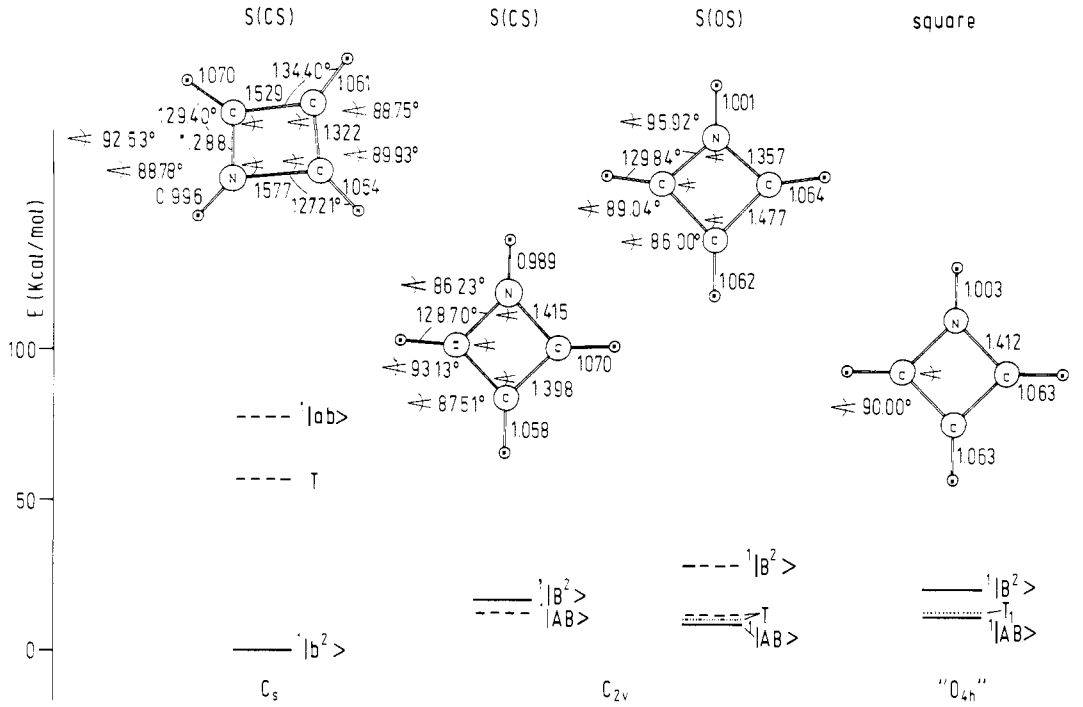

Figure 2. SCF-optimized geometries of protonated azacyclobutadiene **2** [closed-shell S(CS) and open-shell S(OS)] under the symmetry constraints indicated and direct CI energies (cf. Table II). Full lines: the states whose geometry was optimized and is shown. Broken lines: other singlet and triplet states at the same geometry. Dotted lines: the triplet state at its own optimized geometry (very similar to S(OS), see Figure 7). The optimized "D_{4h}" S(CS), S(OS), and T(OS) geometries are very similar, with C–C bond lengths 1.41, 1.40, and 1.41 Å, respectively. The leading configurations in the CI wave function are indicated. Lower case letters: delocalized SCF MO's. Capital letters: localized MO's.

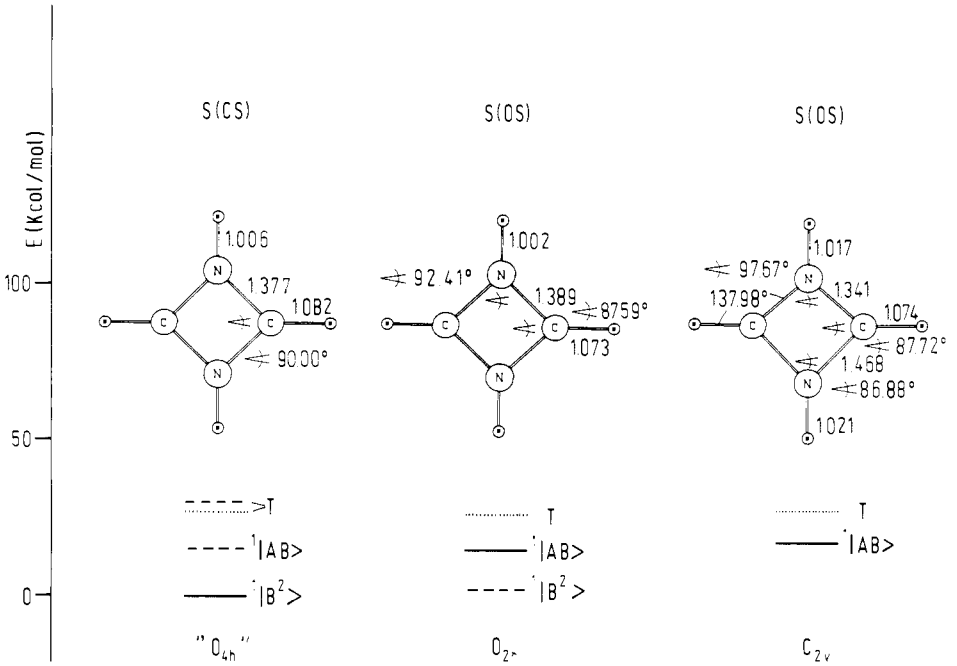

Figure 3. Geometries and energies of protonated 1,3-diazacyclobutadiene **3** (Table III). See caption to Figure 2.

anticipated from a very simple two-electron two-orbital model.[8] In the two-electron basis set $^1|A^2 - B^2\rangle$, $^1|A^2 + B^2\rangle$, and $^1|AB\rangle$, the Hamiltonian matrix is

$$\begin{array}{l} {}^1|A^2 - B^2\rangle: \\ {}^1|A^2 + B^2\rangle: \\ {}^1|AB\rangle: \end{array} \begin{pmatrix} E(T) + 2K' & \delta & 0 \\ \delta & E(T) + 2(K' + K) & \gamma \\ 0 & \gamma & E(T) + 2K \end{pmatrix}$$

where K is the exchange integral between the localized orbitals A and B, $K' = [(J_{AA} + J_{BB})/2 - J_{AB}]/2$, J_{AA}, J_{BB}, and J_{AB} are the Coulomb repulsion integrals between these orbitals, δ is half the energy difference between the configurations $|A^2\rangle$ and $|B^2\rangle$ and provides a measure of the electronegativity difference between orbitals $|A\rangle$ and $|B\rangle$, and γ is a measure of the interaction between these orbitals, approximately equal to twice the resonance integral. $E(T)$ is the energy of the $^3|AB\rangle$ configuration.

At symmetrical geometries, $\gamma = 0$. In **1**, $\delta = 0$ as well and the energies of S_0, S_1, and S_2 are given by the diagonal elements. Since K is very small and K' quite large, the expected order of states in **1** is T ($^3|AB\rangle$), S_0 ($^1|AB\rangle$), S_1 ($^1|A^2 - B^2\rangle$), and S_2 ($^1|A^2 + B^2\rangle$), with the pairs T, S_0 and S_1, S_2 nearly degenerate. These results agree very well with the large-scale CI calculations, except for an inversion of the state order within both nearly degenerate pairs. This is well understood to be due to correlation with the remaining π electrons.[17-20]

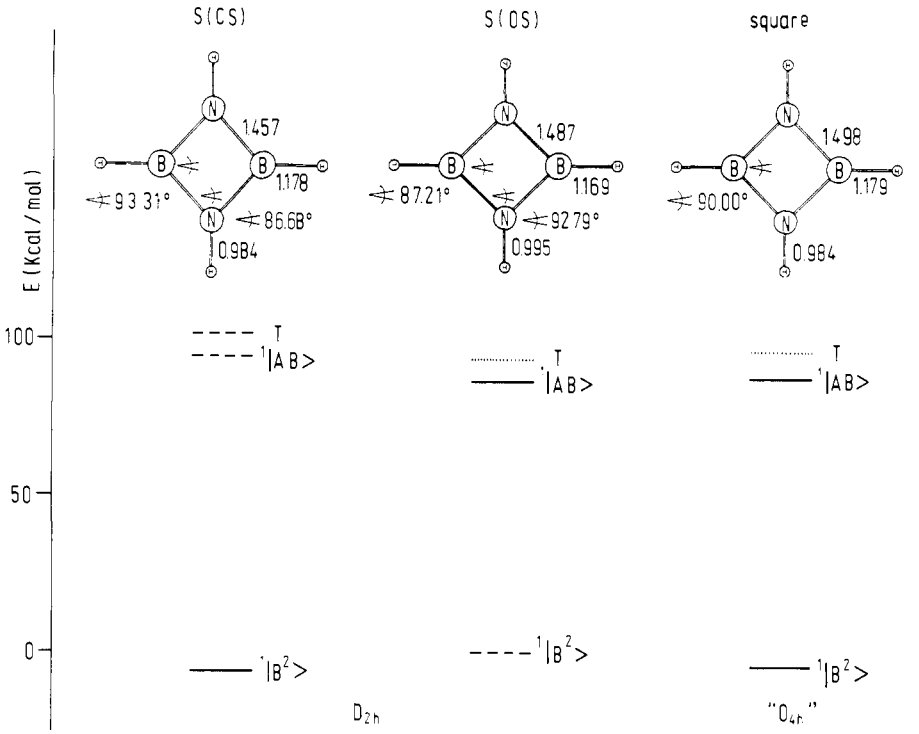

Figure 4. Geometries and energies of 1,3,2,4-diazadiboretidine **4** (Table IV). See caption to Figure 2. Optimized D_{4h} C–C bond lengths: S(CS), 1.460 Å; S(OS) and T(OS), 1.448 Å.

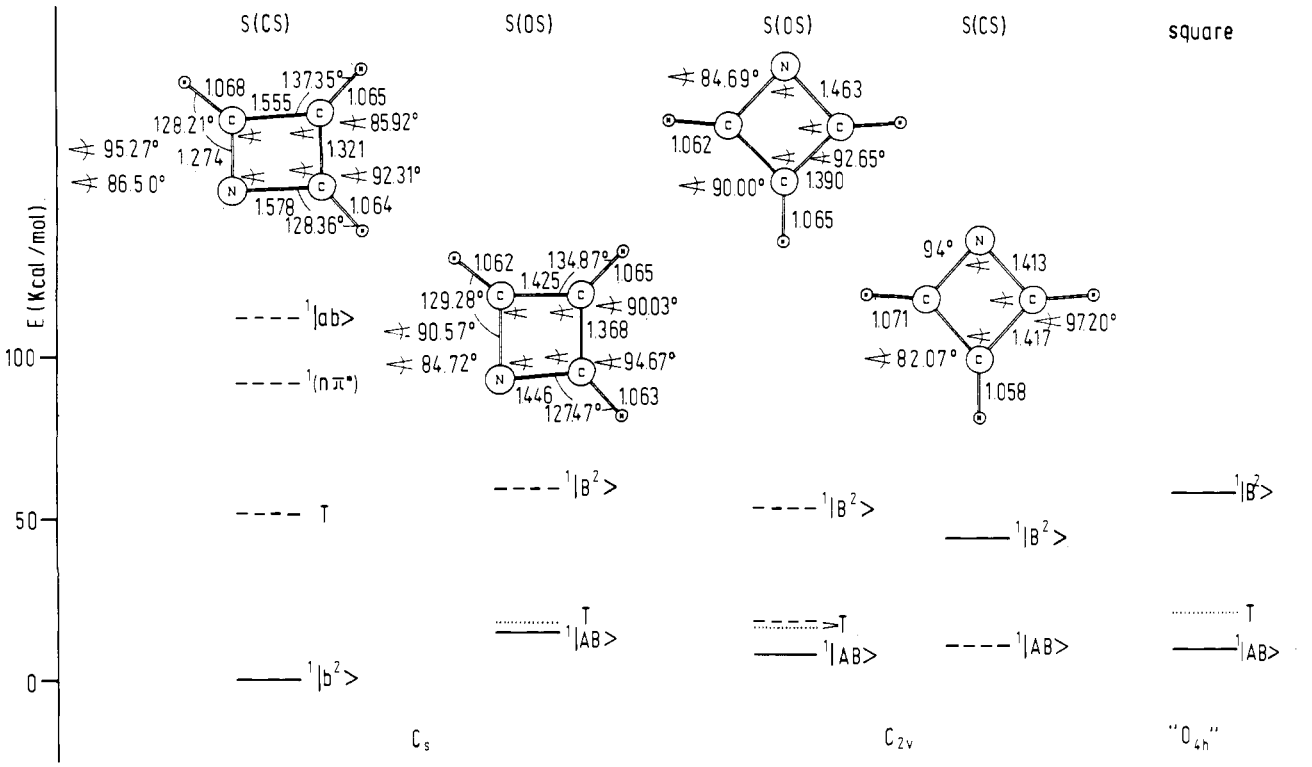

Figure 5. Geometries and energies of azacyclobutadiene **5** (Table V). See caption to Figure 2. Optimized D_{4h} C–C bond lengths: S(CS), 1.417 Å; S(OS), 1.419 Å; T(OS), 1.417 Å.

$$E(S_0),\ E(S_1)\quad \begin{cases} E(T) + 2K \\ E(T) + 2K' + K + (K^2 + \delta^2)^{1/2} \end{cases} \qquad \varphi_0,\ \varphi_1 \begin{cases} {}^1|AB\rangle \\ -\sin\beta\ {}^1|A^2 + B^2\rangle + \cos\beta\ {}^1|A^2 - B^2\rangle \end{cases} \qquad \text{(I)}$$

$$E(S_2)\quad E(T) + 2K' + K + (K^2 + \delta^2)^{1/2} \qquad \varphi_2 = \cos\beta\ {}^1|A^2 + B^2\rangle + \sin\beta\ {}^1|A^2 - B^2\rangle$$

In **2–4**, $\delta \neq 0$: these systems are not perfect biradicals in that they have two only approximately degenerate nonbonding orbitals. This is a "heterosymmetric" perturbation, "even" in the sense of Moffit.[25] Diagonalization yields the results given in (I), where $\beta = {}^1/_2 \tan^{-1}(\delta/K)$. For $\delta \neq 0$, the exact balance in the mixing of the hole–pair configurations ${}^1|A^2\rangle$ and ${}^1|B^2\rangle$ is removed and ${}^1|B^2\rangle$ dominates in the lower of the resulting states. As δ increases, this configuration is greatly stabilized and for $\delta > \delta_0 = 2(K'(K' - K))^{1/2}$ it dominates in the ground-state wave function (strongly heterosymmetric biradicaloids, $\beta = 45°$). For weak perturbations, $\delta < \delta_0$, the ground state is represented by the dot–dot configuration

(25) Moffit, W. J. *Chem. Phys.* **1954**, *22*, 320.

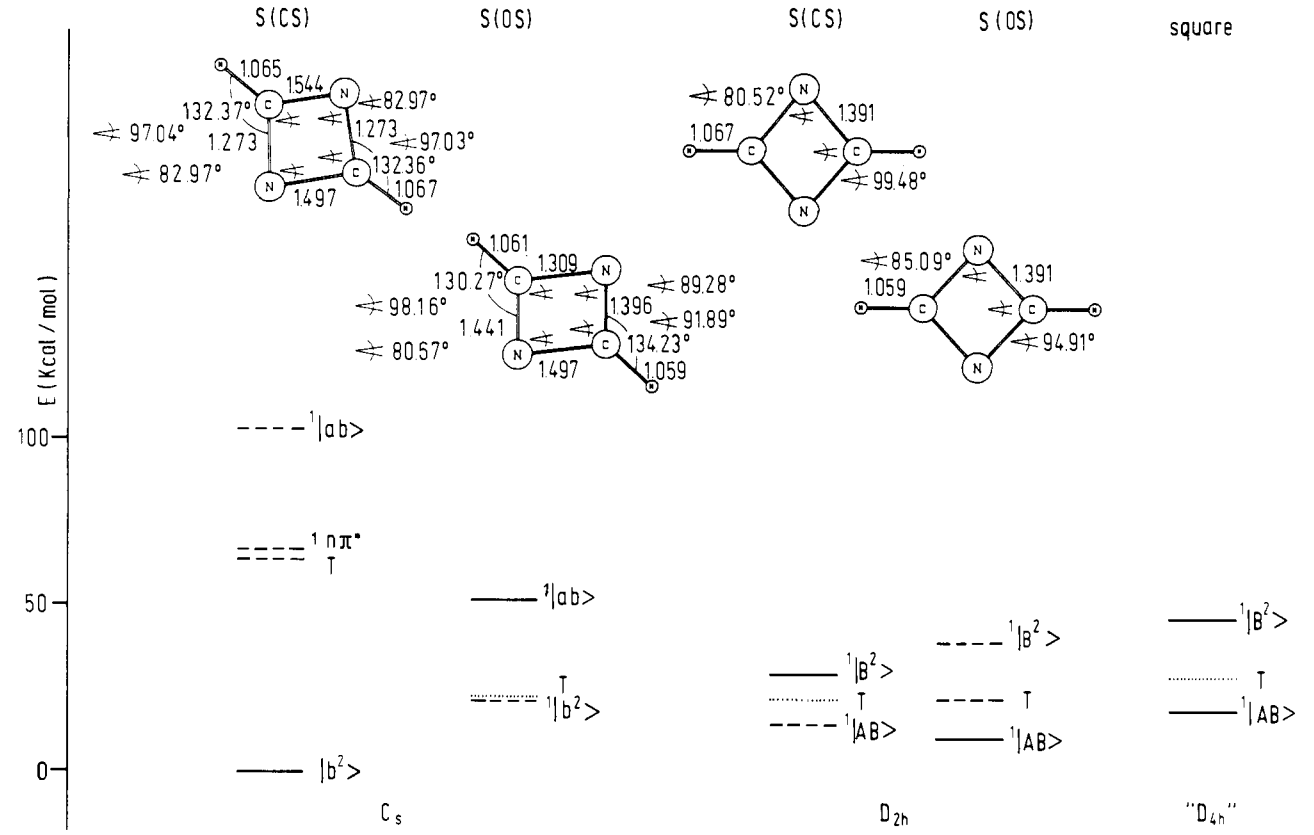

Figure 6. Geometries and energies of 1,3-diazacyclobutadiene **6** (Table VI). See caption to Figure 2. Optimized D_{4h} C–C bond lengths: 1.390 Å.

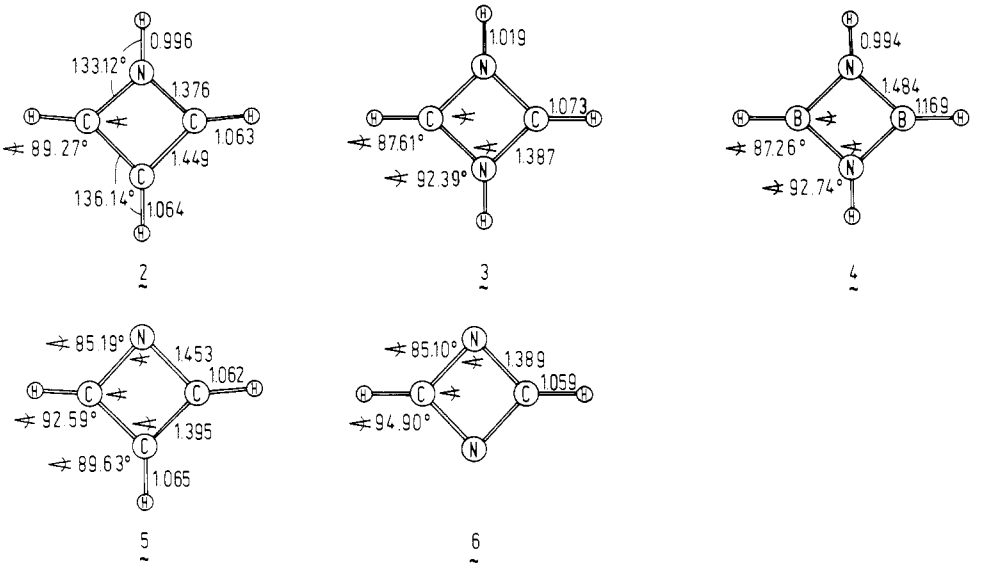

Figure 7. Optimized triplet geometries for **2–6**.

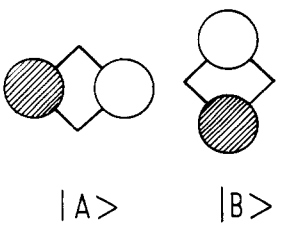

Figure 8. Two nonbonding localized molecular orbitals |A⟩ and |B⟩.

$^1|AB\rangle$ (weakly heterosymmetric biradicaloids). For the critical value of the electronegativity different ($\delta = \delta_0$), S_0 and S_1 are degenerate. As long as the symmetries of the configurations $^1|AB\rangle$, on the one hand, and $^1|A^2\rangle$ and $^1|B^2\rangle$, on the other hand, are different, $\gamma = 0$ and the degeneracy is exact (critically heterosymmetric biradicaloid).

The picture provided by the simple model for the electronic states of **2–4** is in perfect agreement with the results of the ab initio calculations, with respect both to the leading term in the wave functions and to the trends in state energies. clearly, square **1** is a perfect biradical, square **2** a nearly critically heterosymmetric biradicaloid, and **3** and particularly **4** strongly heterosymmetric biradicaloids. the unavoided touching of the S_0 and S_1 states (crossing of the dot–dot and hole–pair states) with increasing electronegativity difference along the two diagonals occurs in the ab initio calculation just as it does in the simple model.

As soon as the symmetry is lowered further, so that $\gamma = 0$ as well (i.e., by adding a heterosymmetric perturbation, "odd" in the sense of Moffit[25]), the $^1|AB\rangle$ configuration can interact with $^1|A^2 + B^2\rangle$ and the degeneracy of S_0 and S_1 is removed in the critical biradicaloid. A nonsymmetric biradicaloid results when γ and

$\delta \neq 0$. The S_0 and S_1 states then no longer touch for any value of δ. For small values of γ, a near toughing is still present; for large γ, all vestiges will be removed. In general, the introduction of a nonvanishing γ stabilizes that singlet state of a biradicaloid in which $^1|AB\rangle$ dominates (pseudo-Jahn–Teller distortion). We can therefore expect the lowest singlet state of weakly and critically heterosymmetrical biradicaloids to stabilize by a symmetry-lowering distortion, while in strongly heterosymmetric biradicaloids such as driving force will be absent.

This result represents bad news for attempts to synthesize weakly or critically heterosymmetric biradicaloids in their S_0 state: the molecules will tend to distort just like perfect biradicals do. For instance, square **1** distorts in the S_0 state to yield one of two possible rectangular forms, and the same will be expected for **2** though not for **3** and **4**. Also these results of the simple model are fully confirmed by the ab initio large-scale CI calculations.

Low-Symmetry Geometries. In **1** the best ground-state geometry is rectangular. The states dominated by $^1|A^2\rangle + {}^1|B^2\rangle$ (S_2) and $^1|A^2\rangle - {}^1|B^2\rangle$ (S_1) are now in the order expected from the simple model, the S_1–S_2 gap has grown from 0.2 (square) to 5.0 kcal/mol, and the S_0–S_1 gap has grown from 47.5 (square) to 89.0 kcal/mol.

As an analogous symmetry-lowering distortion is permitted in the nearly critically heterosymmetric biradicaloid **2**, similar changes occur (Figure 2). A strong mixing of $^1|AB\rangle$ with $^1|B^2\rangle$ causes the near toughing of S_0 and S_1 to be quite strongly avoided, and the gap increases from 3.6 to 77.5 kcal/mol. Clearly, one is observing a Jahn–Teller splitting of the degenerate state of a critically heterosymmetric biradicaloid upon distorting it to a nonsymmetric biradicaloid. The unusual aspect of the situation is the fact that the degeneracy is not imposed by a 3-fold or higher axis of symmetry but is of the "accidental" type.

In the distortion process, the S_0 state has been stabilized by only 13 kcal/mol and the S_1 state destabilized by fully 60.5 kcal/mol. We conclude that, at its equilibrium geometry, **2** is not a critically heterosymmetric biradicaloid in its ground state after all, but geometries characterized by S_0–S_1 degeneracy are available on its lower potential energy surface at energies comparable to activation energies of thermal reactions that are very rapid at room temperature. Such geometries should also be favored in the S_1 state.

As one now proceeds toward the more strongly heterosymmetric biradicaloids **3** and **4**, in which the $^1|B^2\rangle$ configuration dominates the S_0 state of the symmetrical species, the driving force for a rectangular distortion in the ground state is lost. Indeed, ground-state geometry optimization yields an S_0 state of D_{2h} symmetry for **3** and **4** (Figures 3 and 4), and lower symmetry geometries are not favored.

Aza and 1,3-Diaza Analogues of Cyclobutadiene (5, 6). Geometry optimization under the constraint of symmetry higher than C_s yields results quite similar to those obtained for the protonated species in that the lowest states are of π–π^* nature (Figures 5 and 6). However, the electronegativity difference δ for atoms on the two diagonals is now somewhat smaller. At these geometries **5** is a weakly heterosymmetric biradicaloid, while **6** approaches the critical point where S_0 and S_1 should touch. In both cases, the S_0 state wave function is dominated by the $^1|AB\rangle$ configuration. A comparison with **1**–**4** is shown in Figures 1–6 and makes it clear that the S_0–S_1 gap is reduced in **5** relative to **1** and reduced even more in **6**, just as expected from the simple model. At the optimal C_{2v} geometry of the S_1 state of **5**, the S_0–S_1 gap is 33.5 kcal/mol, and at the optimal D_{2h} geometry of the S_1 state of **6**, it is 15.2 kcal/mol.

When the ground-state geometry optimization in **5** and **6** is permitted to proceed to C_s structures, a sizable pseudo-Jahn–Teller distortion to one of two equivalent nearly rectangular structures occurs, as expected for a weakly heterosymmetric biradicaloid. This causes a large increase in the gap between the S_0 and S_1 states of the symmetrical species, just as was the case for **1** and **2**. The stabilization of the S_0 state is 7.4 kcal/mol in **5** and 10.6 kcal/mol in **6**; the destabilization of the upper state is 68.8 kcal/mol in **5** and 83 kcal/mol in **6**. The destabilization is so large that an $^1n\pi^*$ state actually represents the first excited singlet state of **5** and **6** at their ground-state equilibrium geometries. The $^1n\pi^*$ excitation energy is 91.5 kcal/mol in **5** and 67 kcal/mol in **6**.

Once again, in their relaxed ground states, **5** and **6** should not have much biradicaloid character.

Discussion

The excellent agreement between the results derived from the simple two-electron two-orbital model and the ab initio large-scale CI calculations is encouraging and suggests that the model will be qualitatively correct in other situations as well. One such application has been suggested:[8] Since the electronic structure of the π-electron system of **1** is isoelectronic with that of a pericyclic intermediate in a 2s + 2s photochemical cycloaddition reaction,[19] it appears likely that a minimum in the S_1 surface of a face-to-face olefin pair will occur at geometries for which δ is nonzero. Consequently, even the value δ_0 could be reached by a suitable geometrical distortion or by a suitable placement of substituents, resulting in a conical S_0–S_1 intersection and a very efficient return to the ground state. Since a head-to-tail addition arranges the substituents so as to affect δ, while the head-to-head addition does not, this could have significant consequences for photochemical regioselectivity.

Critically heterosymmetric geometries represent the bottom of a funnel in the excited-state S_1 and should provide a rapid return mechanism from the manifold of electronically excited singlet states. This offers an opportunity for "dynamic memory" effects. For instance, in **2** the short and the long C–C bonds of the rectangle acquire equal lengths at the bottom of the funnel, as do those of C–N bonds. The return from the bottom of the funnel to one or the other S_0 minimum should not occur with equal probability and instead should depend on which S_0 minimum vertical excitation originally occurred from. An actual observation of such an effect will be hampered by the presumably rapid tunneling interconversion between the two S_0 minima even at the lowest temperatures.

The situation becomes more favorable when the presence of a counterion and of a polar solvent are taken into account. The most likely location of the counterion and orientation of the solvating molecules will stabilize one of the approximately rectangular structures over the other. Since the interconversion between the two ground-state forms is associated with a considerable degree of intramolecular charge translocation, its rate may be a strong function of the mobility of the counterion and the solvent and may be negligible in a low-temperature glass.

However, the motion of the counterion and the solvent may still be possible during the brief period of return from the S_1 to the S_0 state: as long as the molecule is in the S_1 state, above one of the S_0 minima, the charge distribution corresponds to that of the other S_0 minimum, and there will be a driving force on the counterion and the solvent molecules to move in that direction. A photochemically driven bistable system would result, similar to that we have proposed earlier for the initial step in vision,[8] and somewhat similar to what has been observed in octaethylporphine.[26]

Since tri-*tert*-butylazacyclobutadiene is now known,[27] these conjectures are amenable to experimental verification. Only the absorption spectrum of its unprotonated form has been reported so far.[27] It shows a weak band at 31 250 cm^{-1}, which we assign to the $n\pi^*$ transition, calculated at 32 000 cm^{-1} for the parent **5**, where the blue shift anticipated for the effect of the alkyl substituents is missing.

Acknowledgment. This work was supported by the U.S. National Science Foundation (Grant CHE 8796257) and Deutsche Forschungsgemeinschaft (Grant Bo 627/5-1).

(26) Radziszewski, J. G.; Burkhalter, F. A.; Michl, J. *J. Am. Chem. Soc.* **1987**, *109*, 61.
(27) Vogelbacher, U.-J.; Regitz, M.; Mynott, R. *Angew. Chem. Int. Ed. Engl.* **1986**, *25*, 842.